

Modeling the fast optical transient SN 2019bkc/ATLAS19dqr with a central engine and implication for its origin

Jian-He Zheng (郑见合) and Yun-Wei Yu (俞云伟)

Institute of Astrophysics, Central China Normal University, Wuhan 430079, China
Key Laboratory of Quark and Lepton Physics (Central China Normal University), Ministry of Education, Wuhan 430079, China; yuyw@mail.ccnu.edu.cn

Received 2021 January 24; accepted 2021 March 27

Abstract Modern wide-field high-cadence surveys have revealed the significant diversity of optical transient phenomena in their luminosity and timescale distributions, which led to the discovery of some mysterious fast optical transients (FOTs). These FOTs can usually rise and decline remarkably in a timescale of a few days to weeks, which are obviously much rapider than ordinary supernovae. SN 2019bkc/ATLAS19dqr is one of the fastest detected FOTs so far and, meanwhile, it was found to be unassociated with a host galaxy. These discoveries provide a good chance to explore the possible origins of FOTs. So, we model the light curves of SN 2019bkc in details. It is found that SN 2019bkc can be well explained by the thermal emission of an explosion ejecta that is powered by a long-lasting central engine. The engine could be a spinning-down millisecond magnetar or a fallback accretion onto a compact object. Combining the engine property, the mass of the ejecta, and the hostlessness of SN 2019bkc, we suggest that this FOT is likely to originate from a merger of a white dwarf and a neutron star.

Key words: stars: supernovae — stars: individual (SN 2019bkc)

1 INTRODUCTION

Astronomical transient phenomena, particularly, the ones occurring in extragalactic galaxies usually indicate an extremely huge energy release as a result of catastrophic collapses of massive stars or binaries. Specifically, supernovae (SNe) are undoubtedly the most representative of such transients, which are the primary targets of many current wide-field surveys. Thanks to these modern surveys with their tight cadences, a huge diversity has appeared in the distribution of all SN-like transients in the space of peak luminosity and emission timescale. It is then discovered that some unusual fast optical transients (FOTs) can rise and decline significantly from view in a few days or weeks, which is much more rapider than the typical SNe (Drout et al. 2014; Prentice et al. 2018; Pursiainen et al. 2018; Perley et al. 2019; McBrien et al. 2019; Chen et al. 2020; Gillanders et al. 2020; Prentice et al. 2020). Such fast evolving behaviors indicate that these FOTs probably have origins very and even intrinsically different from normal SN explosions. In any case, within the basic framework of the stellar explosion, the short duration of FOTs could indicate that their progenitors are compact objects or ultra-stripped stars, because the explosion of

these stars can naturally produce a low-mass ejecta of a short photon diffusion timescale (Yu et al. 2015).

The most famous FOT is undoubtedly the kilonova AT2017gfo, which was discovered in the follow-up observations of the gravitational wave (GW) event on 2017 August 17 and had played a crucial role in localizing and identifying the origin of the GW signal (Abbott et al. 2017; Andreoni et al. 2017; Arcavi et al. 2017; Chornock et al. 2017; Coulter et al. 2017; Cowperthwaite et al. 2017; Drout et al. 2017; Evans et al. 2017; Kasliwal et al. 2017; Lipunov et al. 2017; Nicholl et al. 2017; Pian et al. 2017; Smartt et al. 2017; Tanvir et al. 2017; Troja et al. 2017; Utsumi et al. 2017; Valenti et al. 2017). Such kilonova emission was first predicted by Li & Paczyński (1998) and elaborately described by Metzger et al. (2010), as a promising electromagnetic counterpart of a GW event. Following these pioneering works, it is widely suggested that the AT2017gfo emission can be powered by the radioactive decay of heavy r-process elements synthesized during the merger of compact objects (Kasen et al. 2017; Metzger 2017). However, from the detailed modeling of the AT2017gfo data, it can be found that the preconceived radioactive explanation is actually very questionable (Li et al. 2018). Instead, an extra energy source is necessarily required, which can even be dominant

over the radioactive power (Yu et al. 2018; Li et al. 2018). Specifically, such an extra energy source can be provided by a remnant massive neutron star (NS) formed from the merger, as previously suggested by Yu et al. (2013) and Metzger & Piro (2014). The existence of such a post-merger massive NS in the GW170817 event has further been supported by the works of Piro et al. (2019) and Ren et al. (2019).

Fairly speaking, it is not very surprising to find a long-lasting energy engine from an FOT, since such an engine has been widely used to explain some extreme transient phenomena (see Yu et al. 2019a for a brief review), such as superluminous SNe (Woosley 2010; Kasen & Bildsten 2010; Dexter & Kasen 2013) and gamma-ray bursts (Dai & Lu 1998b,a; Dai 2004; Dai et al. 2006; Yu et al. 2010). Just following this knowledge, it has been previously suggested by Yu et al. (2015) that, at least, the FOTs of an ultrahigh luminosity are very likely to be powered by a central engine, where the luminosity is too high to be explained by the radioactive scenario even though all of the explosively-ejected material is supposed to be radioactive. Generally, the nature of the central engine of an FOT could be a spinning-down NS or a fallback accretion onto a compact object, which can evolve from different progenitors.

Recent years, the implementation of modern surveys and the discovery of AT 2017gfo has effectively promoted the discovery of a lot of luminous FOTs (McBrien et al. 2019), among which SN 2019bkc/ATLAS19dqr is the most rapidly declining one that was discovered by Asteroid Terrestrial-impact Last Alert System (ATLAS; Tonry et al. 2018; Chen et al. 2020). This source is the focus of this paper, because of its unprecedented magnitude decline after the peak. In about four days, the luminosity of SN2019bkc decayed by a half. This decline rate is very close to the situation of AT2017gfo (Chen et al. 2020; Prentice et al. 2020). In principle, such a rapid evolution can appear in some ultra-stripped SNe (Tauris et al. 2013) or in the shock breakout emission of some normal or failed SNe, which are however disfavored by the un-association of SN 2019bkc with a host galaxy. Therefore, following the considerations in Yu et al. (2015) and Yu et al. (2018), here we would like to connect SN 2019bkc with a compact object progenitor and model its temporal evolution with a central engine. It is expected that an implication for the origin of SN 2019bkc could be found from the properties of the engine and the explosion ejecta.

2 MODELING THE TEMPORAL EVOLUTION OF SN 2019BKC

2.1 Model Description

For a hot explosion ejecta of a mass M_{ej} and a radius R , the bolometric luminosity of its thermal emission, which

is determined by the heat diffusion in it, can be roughly estimated by (Kasen & Bildsten 2010; Kotera et al. 2013; Yu et al. 2015)

$$L_{\text{bol}} \sim \frac{cE_{\text{int}}}{R\tau}(1 - e^{-\tau}), \quad (1)$$

where c is the speed of light, E_{int} is the internal energy of the ejecta, and $\tau = 3\kappa M_{\text{ej}}/4\pi R^2$ is the optical depth with κ being the opacity. This expression combines two asymptotic properties of the emission as $L_{\text{bol}} = cE_{\text{int}}/(R\tau)$ for $\tau \gg 1$ and $L_{\text{bol}} = cE_{\text{int}}/R$ for $\tau \ll 1$. The evolution of the internal energy is simultaneously determined by the energy conversation as

$$\frac{dE_{\text{int}}}{dt} = L_{\text{ce}} + L_{\text{rad}} - L_{\text{bol}} - 4\pi R^2 p v, \quad (2)$$

where L_{ce} and L_{rad} are the heating rate due to the central engine and the radioactivity, respectively, $p = \frac{1}{3}(E_{\text{int}}/\frac{4}{3}\pi R^3)$ is the radiation-dominated pressure, and v is the expansion velocity of the ejecta which determines the ejecta radius by $dR = v dt$. The expansion velocity can in principle be increased, because of the increase of the kinetic energy E_{k} of the ejecta through the work by the pressure.

For the radioactive power, if it is dominated by the decay of nickels as usual as for typical SNe, then the corresponding heating rate can be given by (Colgate et al. 1980; Arnett 1980)

$$L_{\text{rad,Ni}} = M_{\text{Ni}}[(\epsilon_{\text{Ni}} - \epsilon_{\text{Co}})e^{-t/\tau_{\text{Ni}}} + \epsilon_{\text{Co}}e^{-t/\tau_{\text{Co}}}], \quad (3)$$

where M_{Ni} is the total mass of ^{56}Ni , $\epsilon_{\text{Ni}} = 3.90 \times 10^{10} \text{erg s}^{-1} \text{g}^{-1}$ and $\epsilon_{\text{Co}} = 6.78 \times 10^9 \text{erg s}^{-1} \text{g}^{-1}$, and $\tau_{\text{Ni}} = 8.76$ days and $\tau_{\text{Co}} = 111.42$ days are the lifetimes of the radioactive elements. Alternatively, if the dominant radioactive elements are r-process elements as for typical kilonovae, then we should employ (Korobkin et al. 2012)

$$L_{\text{rad,R}} = 4 \times 10^{18} M_{\text{ej}} \left[\frac{1}{2} - \frac{1}{\pi} \arctan \left(\frac{t - t_0}{\sigma} \right) \right]^{1.3}, \quad (4)$$

with $t_0 = 1.3$ s and $\sigma = 0.11$ s. Meanwhile, the central engine of the FOT can also have two representative natures including (i) a spinning-down NS, which is usually considered to spin at a near-Keplerian frequency and be highly magnetized, and (ii) an accretion of fallback material onto the central compact object. In the former case, the spin-down luminosity of the NS can be estimated by its magnetic dipole radiation power as usual as (Shapiro & Teukolsky 1983)

$$L_{\text{sd}} = L_{\text{sd,i}} \left(1 + \frac{t}{t_{\text{sd}}} \right)^{-2}. \quad (5)$$

In the later case, as usual, we assume simply the accretion luminosity to be proportional to the accretion rate and then

have (Piro & Ott 2011)

$$L_{\text{ac}} = L_{\text{ac,max}} \left[\left(\frac{t}{t_{\text{ac}}} \right)^{-1/2} + \left(\frac{t}{t_{\text{ac}}} \right)^{5/3} \right]^{-1}. \quad (6)$$

Here, the characteristic luminosity $L_{\text{sd},i}$ or $L_{\text{ac,max}}$ and timescale t_{sd} or t_{ac} are taken as free parameters in our calculations. It should be pointed out that, when we use L_{sd} or L_{ac} to determine the energy injection rate L_{ce} in Equation (2), an extra factor of ξ should be multiplied, the value of which is in principle determined by the thermalization efficiency of the energy and also influenced by the possible anisotropic distribution of the energy outflow.

After the bolometric luminosity of the FOT is given, a black-body effective temperature can be given by

$$T_{\text{BB}} = \left(\frac{L_{\text{bol}}}{4\pi R_{\text{ph}}^2 \sigma} \right)^{1/4}, \quad (7)$$

which is crucial for determining the radiation spectrum and then the chromatic luminosities for different filters, where σ is the Stefan-Boltzmann constant and R_{ph} is the photospheric radius. Following Arnett (1982), we define the photospheric radius by

$$R_{\text{ph}} = R - \frac{2}{3}\lambda, \quad (8)$$

where $\lambda(t) = 1/\kappa\rho(t)$ is the mean free path of photons. Obviously, the motion of the photosphere due to the expansion of the ejecta is dependent on the material distribution in the ejecta (see Liu et al. 2018 for a general investigation). For simplicity, we adopt the single power-law density profile in our calculations.

$$\rho(r, t) = \rho(R_i, 0) \left[\frac{R_i - R_{\text{min},i}}{R(t) - R_{\text{min}}(t)} \right]^3 x^{-\delta}, \quad (9)$$

where $R = R_i + vt$ and $R_{\text{min}} = R_{\text{min},i} + v_{\text{min}}t$ are the outmost and inmost radius of the ejecta with R_i and $R_{\text{min},i}$ being their initial values, the dimensionless radius is defined as $x \equiv (r - R_{\text{min}})/(R - R_{\text{min}})$. For such a velocity distribution, the relationship between the leading velocity and the kinetic energy can be written as $v = (2I_M E_k / I_K M_{\text{ej}})^{1/2}$ with $I_M = \frac{1}{3-\delta}$ and $I_K = \frac{1}{5-\delta}$. Finally, when the value given by Equation (8) is smaller than R_{min} , we artificially take $R_{\text{ph}} = R_{\text{min}}$.

2.2 Fitting Results

SN 2019bkc was found to be associated with a galaxy group at redshift ~ 0.02 corresponding to a distance of 89.1 Mpc. This determines its peak luminosity to be around $10^{42} \text{erg s}^{-1}$, which is comparable to that of AT 2017gfo and difficult to be accounted for by a radioactive power. On the one hand, as discussed for AT 2017gfo

Table 1 Parameter Values

Parameters	Units	Spinning-Down NS	Fallback Accretion
$L_{\text{ce},i}$	erg s^{-1}	$9.43^{+0.44}_{-0.87} \times 10^{47}$	$9.54^{+0.36}_{-2.40} \times 10^{48}$
t_{sd} or t_{ac}	s	$4.34^{+0.23}_{-0.10} \times 10^2$	$34.40^{+6.70}_{-0.78}$
M_{ej}	M_{\odot}	$0.35^{+0.02}_{-0.02}$	$0.28^{+0.01}_{-0.02}$
κ	$\text{cm}^2 \text{g}^{-1}$	$0.06^{+0.01}_{-0.01}$	$0.07^{+0.01}_{-0.01}$
E_k	10^{49}erg	$4.32^{+1.20}_{-1.88}$	$5.62^{+0.29}_{-0.67}$
δ	–	$0.96^{+0.03}_{-0.06}$	$0.99^{+0.00}_{-0.01}$

in Li et al. (2018), if the SN 2019bkc emission is purely powered by the decays of r-process elements, then its ejecta mass should be as high as $\sim 1.0 M_{\odot}$ by according to Equation (4). Simultaneously, the opacity is required to be as low as $\sim 0.03 \text{cm}^2 \text{g}^{-1}$, in order to explain the rise time of the emission on the order of a few days by the photon diffusion timescale as $t_{\text{d}} = (3\kappa M_{\text{ej}}/4\pi vc)^{1/2}$. However, in contrast, the typical ejecta masses due to the NS-NS or NS-BH mergers are only around $M_{\text{ej}} = 10^{-4} - 10^{-2} M_{\odot}$ (Hotokezaka et al. 2013) and the corresponding opacity is expected to reach $\sim 10 - 100 \text{cm}^2 \text{g}^{-1}$ due to the synthesis of lanthanides (Tanaka & Hotokezaka 2013). Therefore, the SN 2019bkc emission cannot be powered by the decays of r-process elements. On the other hand, SN 2019bkc is also unlikely to be purely powered by the decay of ^{56}Ni . This is not only because of the unreasonably high requirement on the mass of ^{56}Ni , which is comparable to or even higher than the total mass of the ejecta, but also because the decline time of the emission is actually shorter than the lifetime of ^{56}Ni . Therefore, it is reasonable and necessary to invoke a central engine for explaining the emission characteristics of SN 2019bkc, which has also been previously suggested by Yoshida (2019).

Then, by confronting the engine model with the multi-color observational data of SN 2019bkc, we constrain the model parameters by using the Markov Chain Monte Carlo (MCMC) method (Goodman & Weare 2010). After 5000 steps with 40 “walkers”, we present the parameter constraints in Figure 1 for both models of a spinning-down NS and a fallback accretion. The constrained parameter values are listed in Table 1. Here, besides the central engine, a radioactive power of an amount of $0.002 M_{\odot} ^{56}\text{Ni}$ is still considered, which is necessary for explaining the three late points in *i* band (Chen et al. 2020). For the best-fit parameters, we present the fittings of multi-color light curves of SN 2019bkc in Figure 2. It is shown that both models can in principle be consistent with the observational data. The primary deviation of the models from the data appears in the *i* band. The later the time is, the more serious the deviation will be. This is obviously due to the fact that the de facto emission spectrum can deviate from the black-body spectrum more and more, as the ejecta gradually becomes transparent. This complexity of the emission spectra can be clearly seen from the almost overlap between the *r* and *i* data.

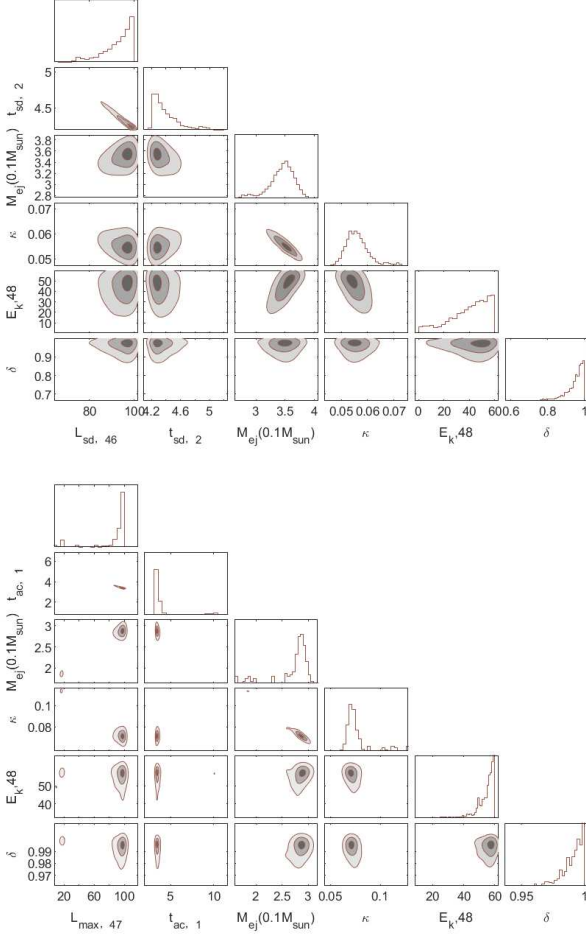


Fig. 1 Observational constraints on the model parameters for the spinning-down NS (*top*) and fallback accretion (*bottom*) models.

Based on the fitting results, if the engine is a spinning-down NS, then we can derive the initial spin period and the dipole magnetic field of the NS to be

$$P_1 = 14.9\xi^{1/2}L_{sd,i,47}^{-1/2}t_{sd,3}^{-1/2}\text{ms} = 7.4\xi^{1/2}\text{ms}, \quad (10)$$

and

$$\begin{aligned} B_p &= 2.2 \times 10^{16}\xi^{1/2}L_{sd,i,47}^{-1/2}t_{sd,3}^{-1} \text{G} \\ &= 1.6 \times 10^{16}\xi^{1/2}\text{G}, \end{aligned} \quad (11)$$

according to the expressions of $\xi L_{sd,i} = 9.4 \times 10^{47}\text{erg s}^{-1}$ and $t_{sd} = 4.3 \times 10^2\text{s}$. This result indicates the post-explosion NS is a millisecond magnetar as expected if $\xi \sim \mathcal{O}(0.1)$, which is well consistent with the previous results found in Yu et al. (2015) for the PS1 transients. Here the value of ξ could be much smaller than 1 because of the following reasons. (i) Drawing lessons from gamma-ray busts and superluminous supernovae, the wind driven by a millisecond magnetar could be highly anisotropic. The majority energy could be collimated within a small cone around the rotational axis and would not influence the thermal emission of the isotropic ejecta. (ii) The

energy released from the isotropic wind component could be partially reflected back into the magnetar wind (Metzger & Piro 2014). (iii) The energy finally injected into the ejecta can only be absorbed and thermalized in the ejecta with a limited efficiency, which is specifically determined by the emission spectrum of the magnetar wind and the energy-dependent opacity of the ejecta (Yu et al. 2019b).

Alternatively, if the engine is a fallback accretion, the maximum accretion rate and the total mass of the fallback material can be estimated to

$$\dot{M}_{ac,max} = L_{ac,max}/c^2 = 5.3 \times 10^{-6}\xi^{-1}M_{\odot}\text{s}^{-1} \quad (12)$$

and

$$M_f \sim \dot{M}_{ac,max}t_{ac} = 1.8 \times 10^{-5}\xi^{-1}M_{\odot}. \quad (13)$$

Meanwhile, the density of the fallback material before it falls back can be estimated to

$$\rho_f \sim (Gt_{ac}^2)^{-1} = 1.3 \times 10^4\text{g cm}^{-3}, \quad (14)$$

since the accretion timescale can be roughly given by the freefall timescale as $t_{ac} \sim (G\rho_f)^{-1/2}$. By combining the values of M_f and ρ_f , we can further obtain the length-scale of the fallback material as

$$R_f \sim \left(\frac{3M_f}{4\pi\rho_f}\right)^{1/3} \sim 1.9 \times 10^8\xi^{-1/3}\text{cm}, \quad (15)$$

which is just smaller than and somewhat comparable to the typical radius $\sim 10^4\text{ km}$ of white dwarfs (Shapiro & Teukolsky 1983).

3 CONCLUSIONS AND DISCUSSION

In this paper, we demonstrate that the fast-evolving luminous emission of SN 2019bkc can be well explained by an explosion that ejects a mass of $\sim 0.3M_{\odot}$ and is lastingly powered by a central engine.

The progenitor of SN 2019bkc is unlikely to be a massive star, because of the deficiency of hydrogen and oxygen features in the spectra and its un-association with a host galaxy. Therefore, the ultra-stripped SN model (Tauris et al. 2013) and the SN shock breakout model are somewhat disfavored. Then, as an alternative natural consideration, the hostlessness of SN 2019bkc could be explained by an NS-NS binary progenitor, the merger of which could lead to the formation of a massive millisecond magnetar. However, this scenario is seriously challenged and even can be ruled out by the required very high mass of the ejecta, even though the ejecta mass can be somewhat increased by a long-lived post-merger NS (Radice et al. 2018).

In comparison, a WD-involved progenitor could be a better choice. Nevertheless, the requirements on the central engine and the ejecta mass still rule out the possibility

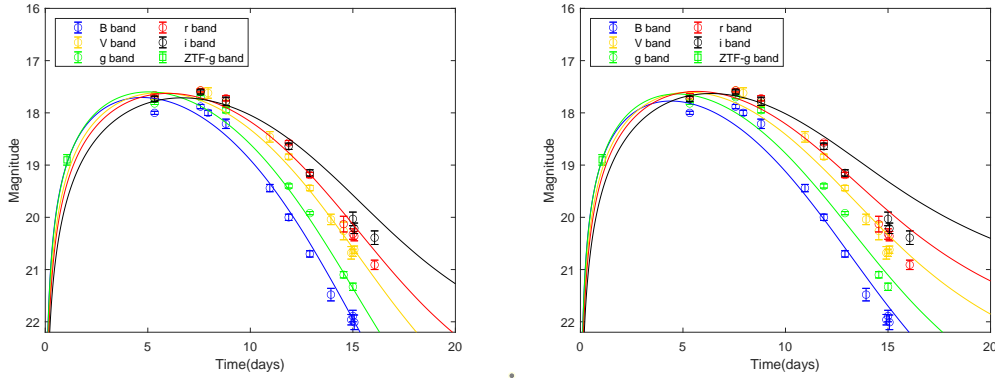


Fig. 2 Fittings to the multi-color light curves of SN 2019bkc with the spinning-down NS model (*left*) and the fallback accretion model (*right*) for the best-fit parameters. The data are taken from [Chen et al. \(2020\)](#) and [Prentice et al. \(2020\)](#). The time origin is set at 2019–02–26 04:48:00 UT (JD 2458540.70).

that SN 2019bkc is an SNIa explosion due to helium-shell detonations on the surface of a sub-Chandrasekhar mass WD ([Bildsten et al. 2007](#); [Shen et al. 2010](#)). Alternatively, SN 2019bkc could originate from the collapse/disruption of a WD, specifically, (i) an accretion-induced collapse of a WD ([Canal & Schatzman 1976](#); [Ergma & Tutukov 1976](#); [Dessart et al. 2006](#); [Yu et al. 2019b,c](#)), (ii) a merger of a WD with an NS or a stellar-mass black hole (BH; [Metzger 2012](#); [McBrien et al. 2019](#)), and (iii) the tidal disruption of a WD by a BH of an intermediate mass of $\sim 10^{2.5} M_{\odot}$ ([Kawana et al. 2020](#)). Fairly speaking, the last scenario could be most likely to generate a sufficiently heavy ejecta. However, it is not sure whether such a system can exist far away from galaxies. In view of this, the existence of an NS in the binary could still be very helpful for understanding the hostlessness of SN 2019bkc, due to the possible high kick velocity of the NS that can lead the binary system to depart from the center of the host before the final merger happens. Therefore, the merger of a WD and an NS could be the most promising origin of SN 2019bkc. After the merger, the remnant NS can have been accelerated to spin at a near-Keplerian frequency due to the accretion of material from the companion WD. Simultaneously, the magnetic field has also been amplified. Then, the transient emission can be primarily powered by the spin-down of this newborn millisecond magnetar. This possible origin of SN 2019bkc makes it similar to another FOT, SN2018kzr, which was discovered by [McBrien et al. \(2019\)](#).

Two open questions still exist. (i) It is not sure whether the WD-NS merger model can explain the Ca-rich lines in the later spectra of SN 2019bkc ([Prentice et al. 2020](#)), in view of that very different abundances of ^{40}Ca have been obtained in different simulations of WD-NS mergers. For example, [Margalit & Metzger \(2016\)](#) found that ^{40}Ca is the most abundant isotopes in a merger of an NS and a helium WD, the mass of which can be not much lower than $0.01 M_{\odot}$. On the contrary, [Zenati et al. \(2019\)](#) claimed that the ejecta of a WD-NS merger should be calcium-deficient.

(ii) The energy injected into the explosion ejecta from the central engine is usually considered to be in the form of high-energy photons such as X-rays that are emitted from the engine outflow. Then, after the ejecta became transparent, this high-energy emission of a luminosity of $10^{40} - 10^{41} \text{erg s}^{-1}$ for months should in principle be detected on the SN 2019bkc’s distance. In other words, as argued by [Prentice et al. \(2020\)](#), the detection of possible X-ray emission can provide a test of the existence of the central engine. However, in fact, a precise prediction of this high-energy emission is actually very dependent on the shock interaction between the engine outflow and the explosion ejecta and also the uncertain shock microphysics. Sometimes, the emission of the engine outflow could be primarily in the UV band and the X-ray emission can be suppressed by an order of magnitude relative to the total power (e.g., see sect. 3 in [Yu et al. 2019b](#)).

Acknowledgements The authors appreciate the anonymous reviewer for helpful comments, Ping Chen and Subo Dong for providing the data, Ziqian Liu for support in computation, and Jinping Zhu, Aming Chen, Liang-Duan Liu, and Jianfeng Liu for their discussions. This work is supported by the Ministry of Science and Technology of the People’s Republic of China (2020SKA0120300) and the National Natural Science Foundation of China (Grant Nos. 11822302 and 11833003).

References

- Abbott, B. P., Abbott, R., Abbott, T. D., et al. 2017, *Phys. Rev. Lett.*, 119, 161101
- Andreoni, I., Ackley, K., Cooke, J., et al. 2017, *PASA*, 34, e069
- Arcavi, I., Hosseinzadeh, G., Howell, D. A., et al. 2017, *Nature*, 551, 64
- Arnett, W. D. 1980, *ApJ*, 237, 541
- Arnett, W. D. 1982, *ApJ*, 253, 785

- Bildsten, L., Shen, K. J., Weinberg, N. N., & Nelemans, G. 2007, *ApJL*, 662, L95
- Canal, R., & Schatzman, E. 1976, *A&A*, 46, 229
- Chen, P., Dong, S., Stritzinger, M. D., et al. 2020, *ApJL*, 889, L6
- Chornock, R., Berger, E., Kasen, D., et al. 2017, *ApJL*, 848, L19
- Colgate, S. A., Petschek, A. G., & Kriese, J. T. 1980, *ApJL*, 237, L81
- Coulter, D. A., Foley, R. J., Kilpatrick, C. D., et al. 2017, *Science*, 358, 1556
- Cowperthwaite, P. S., Berger, E., Villar, V. A., et al. 2017, *ApJL*, 848, L17
- Dai, Z. G. 2004, *ApJ*, 606, 1000
- Dai, Z. G., & Lu, T. 1998a, *Phys. Rev. Lett.*, 81, 4301
- Dai, Z. G., & Lu, T. 1998b, *A&A*, 333, L87
- Dai, Z. G., Wang, X. Y., Wu, X. F., & Zhang, B. 2006, *Science*, 311, 1127
- Dessart, L., Burrows, A., Ott, C. D., et al. 2006, *ApJ*, 644, 1063
- Dexter, J., & Kasen, D. 2013, *ApJ*, 772, 30
- Drout, M. R., Chornock, R., Soderberg, A. M., et al. 2014, *ApJ*, 794, 23
- Drout, M. R., Piro, A. L., Shappee, B. J., et al. 2017, *Science*, 358, 1570
- Ergma, E. V., & Tutukov, A. V. 1976, *Acta Astronomica*, 26, 69
- Evans, P. A., Cenko, S. B., Kennea, J. A., et al. 2017, *Science*, 358, 1565
- Gillanders, J. H., Sim, S. A., & Smartt, S. J. 2020, *MNRAS*, 497, 246
- Goodman, J., & Weare, J. 2010, *Communications in Applied Mathematics and Computational Science*, 5, 65
- Hotokezaka, K., Kiuchi, K., Kyutoku, K., et al. 2013, *Phys. Rev. D*, 87, 024001
- Kasen, D., & Bildsten, L. 2010, *ApJ*, 717, 245
- Kasen, D., Metzger, B., Barnes, J., Quataert, E., & Ramirez-Ruiz, E. 2017, *Nature*, 551, 80
- Kasliwal, M. M., Nakar, E., Singer, L. P., et al. 2017, *Science*, 358, 1559
- Kawana, K., Maeda, K., Yoshida, N., & Tanikawa, A. 2020, *ApJL*, 890, L26
- Korobkin, O., Rosswog, S., Arcones, A., & Winteler, C. 2012, *MNRAS*, 426, 1940
- Kotera, K., Phinney, E. S., & Olinto, A. V. 2013, *MNRAS*, 432, 3228
- Li, L.-X., & Paczyński, B. 1998, *ApJL*, 507, L59
- Li, S.-Z., Liu, L.-D., Yu, Y.-W., & Zhang, B. 2018, *ApJL*, 861, L12
- Lipunov, V. M., Gorbvskoy, E., Kornilov, V. G., et al. 2017, *ApJL*, 850, L1
- Liu, L.-D., Zhang, B., Wang, L.-J., & Dai, Z.-G. 2018, *ApJL*, 868, L24
- Margalit, B., & Metzger, B. D. 2016, *MNRAS*, 461, 1154
- McBrien, O. R., Smartt, S. J., Chen, T.-W., et al. 2019, *ApJL*, 885, L23
- Metzger, B. D. 2012, *MNRAS*, 419, 827
- Metzger, B. D. 2017, *Living Reviews in Relativity*, 20, 3
- Metzger, B. D., & Piro, A. L. 2014, *MNRAS*, 439, 3916
- Metzger, B. D., Martínez-Pinedo, G., Darbha, S., et al. 2010, *MNRAS*, 406, 2650
- Nicholl, M., Berger, E., Kasen, D., et al. 2017, *ApJL*, 848, L18
- Perley, D. A., Mazzali, P. A., Yan, L., et al. 2019, *MNRAS*, 484, 1031
- Pian, E., D’Avanzo, P., Benetti, S., et al. 2017, *Nature*, 551, 67
- Piro, A. L., & Ott, C. D. 2011, *ApJ*, 736, 108
- Piro, L., Troja, E., Zhang, B., et al. 2019, *MNRAS*, 483, 1912
- Prentice, S. J., Maguire, K., Smartt, S. J., et al. 2018, *ApJL*, 865, L3
- Prentice, S. J., Maguire, K., Flörs, A., et al. 2020, *A&A*, 635, A186
- Pursiainen, M., Childress, M., Smith, M., et al. 2018, *MNRAS*, 481, 894
- Radice, D., Perego, A., Hotokezaka, K., et al. 2018, *ApJL*, 869, L35
- Ren, J., Lin, D.-B., Zhang, L.-L., et al. 2019, *ApJ*, 885, 60
- Shapiro, S. L., & Teukolsky, S. A. 1983, *Black Holes, White Dwarfs, and Neutron Stars: the Physics of Compact Objects* (A Wiley-Interscience Publication, New York: Wiley)
- Shen, K. J., Kasen, D., Weinberg, N. N., Bildsten, L., & Scannapieco, E. 2010, *ApJ*, 715, 767
- Smartt, S. J., Chen, T. W., Jerkstrand, A., et al. 2017, *Nature*, 551, 75
- Tanaka, M., & Hotokezaka, K. 2013, *ApJ*, 775, 113
- Tanvir, N. R., Levan, A. J., González-Fernández, C., et al. 2017, *ApJL*, 848, L27
- Tauris, T. M., Langer, N., Moriya, T. J., et al. 2013, *ApJL*, 778, L23
- Tonry, J. L., Denneau, L., Heinze, A. N., et al. 2018, *PASP*, 130, 064505
- Troja, E., Piro, L., van Eerten, H., et al. 2017, *Nature*, 551, 71
- Utsumi, Y., Tanaka, M., Tominaga, N., et al. 2017, *PASJ*, 69, 101
- Valenti, S., Sand, D. J., Yang, S., et al. 2017, *ApJL*, 848, L24
- Woosley, S. E. 2010, *ApJL*, 719, L204
- Yoshida, S. 2019, *Research Notes of the American Astronomical Society*, 3, 112
- Yu, Y.-W., Chen, A., Dai, Z.-G., et al. 2019a, in *American Institute of Physics Conference Series*, 2127, Xiamen-CUSTIPEN Workshop on the Equation of State of Dense Neutron-Rich Matter in the Era of Gravitational Wave Astronomy, 020024
- Yu, Y.-W., Chen, A., & Li, X.-D. 2019b, *ApJL*, 877, L21
- Yu, Y.-W., Chen, A., & Wang, B. 2019c, *ApJL*, 870, L23
- Yu, Y.-W., Cheng, K. S., & Cao, X.-F. 2010, *ApJ*, 715, 477
- Yu, Y.-W., Li, S.-Z., & Dai, Z.-G. 2015, *ApJL*, 806, L6
- Yu, Y.-W., Liu, L.-D., & Dai, Z.-G. 2018, *ApJ*, 861, 114
- Yu, Y.-W., Zhang, B., & Gao, H. 2013, *ApJL*, 776, L40
- Zenati, Y., Perets, H. B., & Toonen, S. 2019, *MNRAS*, 486, 1805